AUTONOMOUS ARTIFICIAL SATELLITE ORBIT DETERMINATION IN REAL-TIME USING SINGLE FREQUENCY GPS MEASUREMENTS

Ana Paula Marins CHIARADIA[‡]
Hélio Koiti KUGA[*]
Antonio Fernando Bertachini de Almeida PRADO[*]

[‡]*Department of Mathematics - ITA/CTA*
CEP: 12228-901 - São José dos Campos -SP - Brazil
Phone: ++ 55 12 3947 5949 - Fax: ++55 12 3947 58 45
chiara@ief.ita.br

**INPE – Space Mechanics and Control Division*
Av. dos Astronautas, 1758
CEP: 12 227-010 - São José dos Campos - SP - Brazil
Tel: ++55 12 3945 6199   Fax: ++55 12 3945 6226
hkk@dem.inpe.br, prado@dem.inpe.br

ABSTRACT *- The main goal of this work is to assess, through realistic computational simulations, the attainable real time accuracy provided by single frequency GPS receivers when determining orbits of artificial satellites. A simplified and compact algorithm with low computational burden aiming accuracies around tens of meters for orbit determination using the GPS is developed. To validate the procedure, real data of the Topex/Poseidon satellite were used. For several test cases, the real-time position and velocity errors were ranging between 15 to 20 m and 0.014 to 0.018 m/s along a day, respectively, either with or without Selective Availability (SA).*

KEYWORDS: GPS, Kalman filtering, autonomous orbit determination, single frequency GPS measurements, real-time navigation.

INTRODUCTION

With the advances of technology, nowadays the single frequency GPS (Global Positioning System) receivers provide a good basis to achieve fair precision at relatively low cost in the orbit determination of artificial satellites. The main goal of this work is to test, through realistic computational simulations, the real time attainable accuracy provided by such a receiver when determining orbits of artificial satellites.

Within this scope, a simplified and compact algorithm with low computational burden providing an accuracy around tens of meters for artificial satellite orbit determination in real-time, using the GPS, is developed. This accuracy level is enough for satellites to navigate autonomously and may be used to compute onboard correction orbit maneuvers [1].

DESCRIPTION OF ALGORITHM

A state vector with a minimum set of solve-for variables namely, the position and velocity components, bias, drift and drift rate of the GPS receiver clock, is estimated by a non-linear extended Kalman filter. The coefficients that represent the bias, drift, and drift rate of the GPS receiver clock are estimated as parameters. The simple fourth order Runge-Kutta numerical integrator is used to integrate stepwise the differential equations of motion. Several studies are developed including different numerical integration schemes, Runge-Kuttas of different orders, step size magnitudes, and geopotential harmonic model truncations. In these studies, the equations of motion accounting only for the perturbations due to the geopotential up to 10th order and degree of the JGM-2 model harmonic coefficients have been enough to achieve the accuracy of tens of meters. On the other hand, the state error covariance matrix is propagated through the transition matrix, which is calculated in an optimized analytical way. Within a single integration step, only the two-body Keplerian motion is considered to compute the transition matrix. The single frequency GPS pseudo-range measurements in L1 frequency are used as observation ones. The measurements are corrected for GPS satellite and receiver clocks offsets, relativistic effect, and travel time.

Preliminary studies were carried out to check the impact of the ionospheric effect as well as the non-inclusion of J_2 effect in the transition matrix in the estimated orbit accuracy. It could be concluded that the ionospheric effect could be neglected for satellites with altitudes above 1000 km from the Earth. The analytical J_2 effect inclusion in the transition matrix did not provide meaningfully better results when precision versus processing time is analyzed. Such studies yielded the support to the simplified models adopted in this work.

Force Model and Numerical Integration

To choose a simplified force model adopted in this work, the following factors were considered: generality, orbit accuracy and computational cost for orbit determination in an onboard real time environment. Therefore, only forces due to the Earth gravitational field were implemented.

The considered harmonic coefficients of the Earth's geopotential field are set up to order and degree 10 of JGM-2 model according to studies developed in [2], without overloading the processing time.

The acceleration and the related partial derivatives matrix are computed through the recurrence relations according to [3] in Earth-fixed (EF) coordinates. The coordinates transformation from True of Date (ToD) to Pseudo-Earth fixed equator and prime meridian (PEF) takes into account the Earth sideral rotation, but the polar motion is neglected in this work.

The integration of the satellite's motion equation is performed using the simple 4th order Runge-Kutta (RK4) algorithm. This algorithm is implemented without any mechanism of step adjustment or error control. The RK4 is considered an adequate numerical integrator due to its simplicity, fair accuracy, low truncation error, and low computational burden. An initialization procedure is not necessary and the step size is quite easy to change. The 30-second integration step interval is used throughout.

Measurement Model

Only the code pseudorange in L1 frequency is used to determine the satellite orbit providing the accuracy required by a mission as in this work. The considered errors in the code pseudorange measurements are the GPS satellite and receiver clock offsets. Refs. [4] and [2] studied the need of considering the ionospheric correction model. It has been concluded that the ionospheric effect (around 3-6 meters) does not affect significantly the final accuracy of the orbit. In this way, it will be neglected once the goal is not to achieve high precision (around centimeters). In high precision and onboard applications, some ionospheric correction for single frequency should be applied, but this may add some complexity if we need to implement a better ionospheric model.

The equation of the code pseudorange in L1 frequency is given by:

$$\rho_c = \rho + c[\Delta t_{GPS}(t) - \Delta t_u(t)], \tag{1}$$

where ρ_c is the code pseudorange in L1, c is the vacuum speed of light, Δt_{GPS} is the GPS satellite clock offset, Δt_u is the receiver clock offset, t is the observation instant in GPS time, and ρ is the geometric range given by:

$$\rho = \sqrt{(x_{GPS} - x)^2 + (y_{GPS} - y)^2 + (z_{GPS} - z)^2} \tag{2}$$

where x, y, and z are the positional states of the user satellite at the reception time (in GPS time) and x_{GPS}, y_{GPS}, and z_{GPS} are the positional states of the GPS satellite at the transmission time (in GPS time), corrected for light time delay.

The second term on the right side of the Eq. (1) is the clock bias that represents the combined clock offsets of the satellite and of the receiver with respect to the GPS time. Each GPS satellite contributes with one clock bias. The information for the GPS satellite clocks is known and transmitted via the navigation message in the form of three polynomial coefficients with a reference time t_{oc}. The clock correction of the GPS satellite for the epoch t is:

$$t = t_{GPS} - \Delta t_{GPS}, \tag{3}$$

$$\Delta t_{GPS} = a_{f0} + a_{f1}(t - t_{oc}) + a_{f2}(t - t_{oc})^2 + \delta_R^{GPS}, \tag{4}$$

and

$$\delta_R^{GPS} = \frac{2}{c^2}\sqrt{a\mu}\, e \sin E, \tag{5}$$

where t_{GPS} is the spacecraft code phase time at the message transmission time in seconds; a_{f0},, a_{f1}, and a_{f2} are bias, drift, and drift rate of GPS satellite clock, respectively; t_{oc} is the reference time, in seconds, measured from the GPS time weekly epoch; δ_R is a small relativistic correction of the GPS satellite clock caused by the orbital eccentricity e; a is the semi-major axis of the orbit; μ is the Earth's gravitational constant; and E is the eccentric anomaly.

The relativistic effect is included in the clock polynomial broadcast via the navigation message, where the time dependent eccentric anomaly E is expanded into a Taylor series. If a more accurate equation is required, the relativistic effects must be subtracted from the clock polynomial coefficients. The polynomial coefficient a_{f0}, a_{f1}, and a_{f2} are transmitted in units of sec, sec/sec, and sec/sec^2, respectively. The clock data reference time t_{oc} is also broadcast. The value of t_{GPS} must account for the beginning or the end-of-week crossovers. The user may approximate t by t_{GPS} in Eq. (3). The user clock offset is part of the estimated state vector given by [5]:

$$c\Delta t_u = b_0 + b_1 \Delta T + b_2 \Delta T^2 + \delta_R^{USER} \tag{6}$$

where b_0,, b_1 and b_2 are the bias, drift, and drift rate of the user clock, and ΔT is the elapsed time since the instant of the first measurement. The relativistic effect in the user clock is calculated by using the best available estimated state vector in the epoch.

GPS Travel and Reception Times

The computation of the geometric range, ρ, is required for both pseudorange and carrier phase processing. The GPS position coordinates are used at the instant of emission. However, the reception time is used to compute it. Then, this time is corrected subtracting the travel time of signal to obtain the emission time. Therefore the travel time is computed through an iterative process that starts assuming an average value for the travel time τ. Next, the GPS position for the epoch (t - τ) is interpolated and then, the geometric range is computed, which can be used to reconstruct the travel time by [6]:

$$\tau = \frac{\rho}{c}\,. \tag{7}$$

The light-time iteration is usually performed in an inertial system with position vector $\boldsymbol{x} = (x, y, z)$ and the GPS satellite position vector $\boldsymbol{x_{GPS}} = (x_{GPS}, y_{GPS}, z_{GPS})$. Therefore the positions from inertial to the Earth-fixed WGS84 system or vice-versa are needed. So, the signal path is given as [7]:

$$\rho = \boldsymbol{R}^{WGS}(t)\big(\boldsymbol{r_{GPS}}(t-\tau) - \boldsymbol{r}(t)\big) \tag{8}$$

where $\boldsymbol{R}^{WGS}$ is the rotation matrix from inertial to Earth-fixed WGS-84 system. Making use of the approximation

$$\boldsymbol{R}^{WGS}(t) \approx \boldsymbol{R}_z(\omega_e\tau)\boldsymbol{R}^{WGS}(t-\tau) \tag{9}$$

where ω_e is the Earth's rotation rate, the inertial position of the GPS satellite may be substituted by the corresponding Earth-fixed position:

$$\boldsymbol{r}_{GPS}^{WGS}(t-\tau) = \boldsymbol{R}^{WGS}(t-\tau)\boldsymbol{r}_{GPS}(t-\tau)\,. \tag{10}$$

This yields

$$\rho = c\tau = \left|\boldsymbol{R}_z(\omega_e\tau)\boldsymbol{r}_{GPS}(t-\tau) - \boldsymbol{r}^{WGS}(t)\right| \tag{11}$$

in the Earth-fixed reference frame.

If the discrepancy between the first and second approximation of τ is greater than a specified criterion, the iteration is repeated, i.e., a new satellite position is interpolated and a new distance is computed, and so on. Generally, a couple of iterations are sufficient.

This computation is not affected by the receiver clock error Δt_u and the satellite clock error Δt_{sv}. However, the ionosphere troposphere, hardware, and multipath corrupt the computed nominal emission time. All of these effects are neglected in the present context. The same process corrects the reception time as well.

Estimation Technique

The standard Kalman filter algorithm is used to estimate the spacecraft orbit onboard. This filter is robust, with easy implementation for application in real-time, not requiring iteration on the data collected previously, and being able to provide the current orbit in real time.

The extended Kalman filter is a version applicable to non-linear problems and is composed by time-update and measurement-update cycles. The time-update phase updates the state and the covariance matrix along the time using the dynamical equations.

In this work, the estimated state vector is given by:

$$\boldsymbol{x} = (\boldsymbol{r}, \boldsymbol{v}, \boldsymbol{b})^T\,, \tag{12}$$

where $\boldsymbol{r} = (x,y,z)^T$ and $\boldsymbol{v} = (\dot{x}, \dot{y}, \dot{z})^T$ are the spacecraft's position and velocity vectors, $\boldsymbol{b} = (b_0, b_1, b_2)^T$, where b_0, b_1, b_2 are bias, drift, and drift rate of the receiver clock, respectively, and t is the instant of integration. All coordinates refer to the ToD (True of Date) system.

The used algorithm can be found in [8-9]. The details of implementation can be found in [10]**.**

The state error covariance matrix is propagated through the transition matrix. The conventional filter is implemented calculating only the upper triangular part of the state error covariance matrix. The other elements are obtained imposing symmetry to the matrix. The lack of symmetry is one of the highest sources of truncation error per Kalman filter cycle [11].

One method to avoid the problem of the high computational cost and the extended analytical expressions of the transition matrix consists of propagating the state vector using the complete force model and, then, to compute the transition matrix using a simplified force model. The analytical calculation of the transition matrix of the Keplerian motion is a reasonable approximation when only short time intervals of the observations and reference instant are involved [12]. On the other hand, the inclusion of the J_2 (Earth flattening) effect in the transition matrix can be done approximately adopting the Markley's method [13].

Ref. [2] studied these two methods. The methods were evaluated according to accuracy, processing time, and handling complexity of the equations for two kinds of orbits. It has been concluded that the analytical Keplerian motion model, which was developed in [12], is still a better-suited force model to be adopted in the evaluation of a general-purpose state transition matrix.

SIMULATIONS

In order to test under realistic conditions the algorithm, the data of the Topex/Poseidon (T/P) satellite is used. This satellite carries a dual frequency receiver GPS onboard experimentally to test the ability of the GPS to provide precise orbit determination (POD).The following files are used:

- The T/P observation files that broadcast the code and carrier pseudoranges measurements in two frequencies in 10-second GPS time steps and are provided by GPS Data Processing Facility of the Jet Propulsion Laboratory (NASA) in Rinex II ASC format;
- The T/P Precise Orbit Ephemeris (POE) files that are generated by the Jet Propulsion Laboratory (JPL) in one minute UTC (Universal Coordinated Time) time steps in the Inertial True of Date coordinates; and
- The broadcast GPS navigation message file in Rinex II ASC format provided by Crustal Dynamics Data Information System (CDDIS) of the Goddard Space Flight Center (NASA).

The position and velocity estimates provided by the algorithm are compared against the T/P POE. The T/P POE is claimed to estimate T/P position with accuracy better than 15 cm. The states in the POE are provided in one minute UTC time steps in ToD coordinates. But, the T/P GPS measurements are provided in 10 seconds of GPS time. According to IERS (International Earth Reference System), the difference between the UTC and GPS time is approximately an integer number of seconds, increasing timely with the introduction of leap seconds. For example, for 1993, the difference was 9 seconds.

However, in the process of the orbit determination, the state is estimated in 30-second intervals in UTC time with transmission and reception time correction. As a consequence, these data instants are not coincident. Therefore, it was necessary to interpolate the states through an interpolation (Polint) subroutine [14]. With this approach, the mean errors of the interpolated states are 0.068 m and 2.5×10^{-4} m/s for position and velocity, respectively, which does not add any significant bias to the accuracy evaluation of the results.

Some parameters to be used in evaluating of algorithm in the tests were defined. The actual position error is given by:

$$\Delta \boldsymbol{r} \equiv \left[\sum_{i=1}^{3} \left(x_i - \hat{x}_i \right)^2 \right]^{\frac{1}{2}}, \tag{13}$$

where x_i and $\hat{x}_i$, $i = 1,2,3,$ are the components of the reference (POE) and estimated position vectors, respectively. The estimated position error is given by:

$$\Delta \hat{\boldsymbol{r}} = \left[\sum_{i=1}^{3} \boldsymbol{P}_{ii} \right]^{\frac{1}{2}}, \tag{14}$$

where P_{ii}, $i = 1,2,3$, represents the values of diagonal elements of the state error covariance matrix corresponding to position components. The actual velocity error is given by:

$$\Delta \boldsymbol{v} \equiv \left[\sum_{i=4}^{6} \left(x_i - \hat{x}_i \right)^2 \right]^{\frac{1}{2}}, \tag{15}$$

where x_i and $\hat{x}_i$, i = 4,5,6, are the components of the reference (POE) and estimated velocity vectors, respectively. The estimated velocity error is given by:

$$\Delta \hat{\boldsymbol{v}} = \left[\sum_{i=4}^{6} \boldsymbol{P}_{ii} \right]^{\frac{1}{2}}, \tag{16}$$

where P_{ii}, $i = 4,5,6$, represents the values of diagonal elements of the state error covariance matrix for the velocity components. And, the residual is given by:

$$\Delta \boldsymbol{\rho} = \boldsymbol{z} - \boldsymbol{\rho}_c , \tag{17}$$

where $\boldsymbol{z}$ e $\boldsymbol{\rho_c}$ are the observed and calculated pseudorange measurements, respectively.

The algorithm is analyzed and tested using 8 complete days of data. Figs. 1 and 2 show the real and filtered position and velocity errors in m and m/s, with SA (Selective Availability) off and on, respectively. These figures show the results for a typical day of filtering. Fig. 3 shows the typical behavior of the pseudorange residuals for all tests. Figs. 4 and 5 show the histogram and normal distribution of the residuals. Table 1 shows the statistical errors for position and velocity vectors as well as the residual for all tests

It can be noted that, for all the days tested, the real position and velocity errors are less than the estimated position and velocity errors by the filter. It shows the conservative behavior of the filter. In all cases, the filtering takes around one hour to stabilize the covariance and the error. The position accuracy with SA off (11/18/1993 and 11/19/1993) or on (other days) is from 15 to 20 m with standard deviation from 6 to 10 m. And the velocity accuracy is from 0.014 to 0.018 m/s with standard deviation from 0.006 to 0.009 m/s, as shown in Table 1.

Through Figs. 4 and 5 and Table 1, it can be noted that the residuals present normal distribution with mean zero and standard deviation around 23 m, except for days 18-19. In November 18th and 19th 1993, the SA was off and the standard deviation of the residuals was down to around 13.3 m. This fact shows how SA affects the statistics of the residuals, although the state estimates does not show significant degradation.

CONCLUSIONS

The main goal of this work was to achieve accuracy around tens of meters along with minimum computational cost when determining, in real time, artificial satellite orbits, considering an onboard simplified model. To develop it, the single frequency GPS measurements are modelled, considering the effects of the clock offsets of the GPS and user satellites, and user relativistic effects.

The algorithm was tested with real data from a satellite with GPS receiver onboard. The satellite orbit is estimated using the developed algorithm with a good accuracy and at low computational burden. The algorithm uses a large 30 seconds step-size of propagation (10 second step-size can be used as well), the geopotential model up to order and degree 10, and the analytical computation of the transition matrix considering the Keplerian motion. The obtained position accuracy is better than 20 m with either SA on or off. The results were considered statistically consistent and the tunned Kalman filter behaved as expected.

ACKNOWLEDGEMENT

The authors wish to express their appreciation for the support provided by INPE (Brazilian Institute for Space Research).

REFERENCES

[1] Orlando, V.; Kuga, H.K. Analysis of an Autonomous Orbit Control Concept Using GPS. *Journal of the Brazilian Society of Mechanical Sciences*, Vol. XXI, Special Issue, Feb. 1999, p. 52-59.

[2] Chiaradia, AP.M. *Autonomous artificial satellite orbit determination and maneuver in real-time using single frequency GPS measurements*. INPE, São José dos Campos, 200p. Ph.D. Dissertation. 2000. (In Portuguese).

[3] Pines, S. Uniform representation of the gravitational potential and its derivatives. *AIAA Journal*, 1973, Vol. 11, no. 11.

[4] Chiaradia, A.P.M.; Kuga, H.K.; Prado, A. F.B.A. Investigation on ionospheric correction models for GPS signals. *Advances in Space Dynamics*. In: A.F.B.A. Prado (Editor), p. 214-219, INPE, 2000.

[5] Chiaradia, A.P.M.; Gill, E.; Montenbruck, O.; Kuga, H.K.; Prado, A.F.B.A. *Algorithms for on-board orbit determination using GPS - OBODE-GPS*. Wessling, Germany, DLR, 2000. 43p. (DLR – GSOC TN 00-04).

[6] Leick, A. *GPS Satellite Surveying*. 2nd edition. John Wiley & Sons, 1995. 560p.

[7] Montenbruck, O.; Gill, E. *Satellite Orbits – Models, Methods, and Applications.* Springer Verlag, Heidelberg, 2000.

[8] Gelb, A., Kasper Jr., J.F., Nash Jr., R.A., Price, C.F.; Sutherland Jr., A.A.; *Applied Optimal Estimation*. The M.I.T. Press, England, 1974. 374p.

[9] Maybeck P.S. *Stochastic Models, Estimation, and Control*. Vol. 1, Academic Press, London, 1979. 423p.

[10] Chiaradia, A.P.M.; Kuga, H.K.; Prado, A.F.B.A. Investigation of simplified models for orbit determination using single frequency GPS measurements*.* *RBCM - Journal f the Brazilian Society Mechanical Sciences*, 1999, v. XXI - Special Issue, p. 165-172.

[11] Kuga, H. K. *Orbit determination of Earth artificial satellites through state estimation techniques combined with smoothing techniques.* INPE, São José dos Campos, 249p., Ph.D. Dissertation. 1989 (INPE-4959-TDL/079). (In Portuguese).

[12] Kuga, H. K. *Transition matrix of the elliptical Keplerian motion.* INPE, São José dos Campos, 1986 (INPE-3779-NTE/250). (In Portuguese).

[13] Markley, F.L. Approximate cartesian state transition matrix. *The Journal of the Astronautical Sciences.* 1986, Vol. 34, no. 12, p. 161-169.

[14] Press, H.W.; Flannery, B.P.; Teukolsky, S.A.; Vetterling, W.T. *Numerical Recipes*. Cambridge University Press, 3rd edition, 1987. 818p.

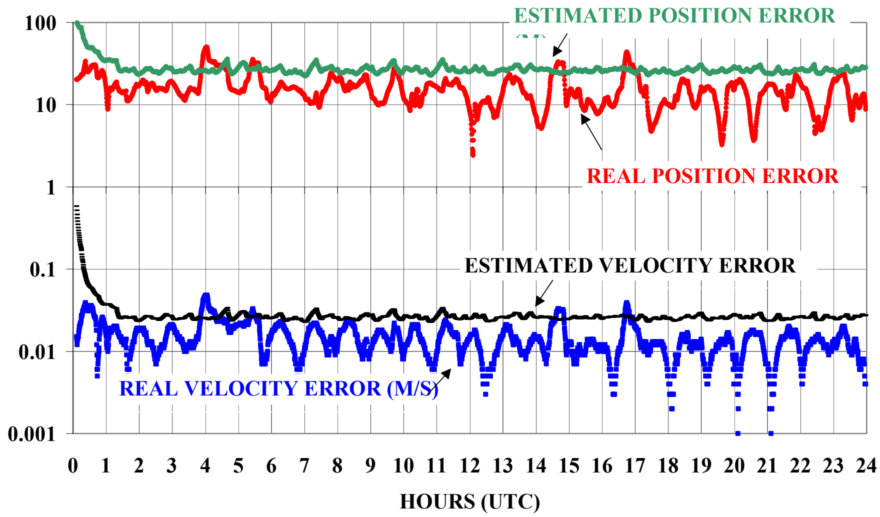

Fig. 1 - Estimated and real position error with SA off

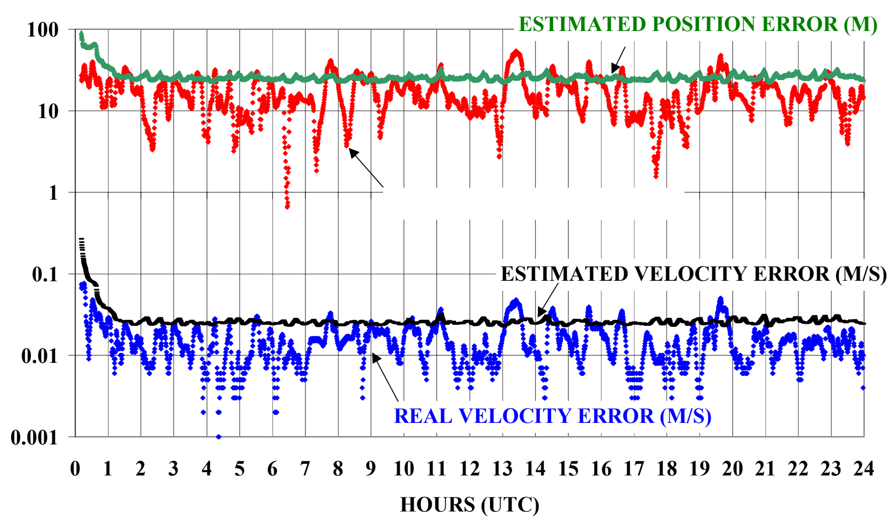

Fig. 2 - Estimated and real position error with SA on

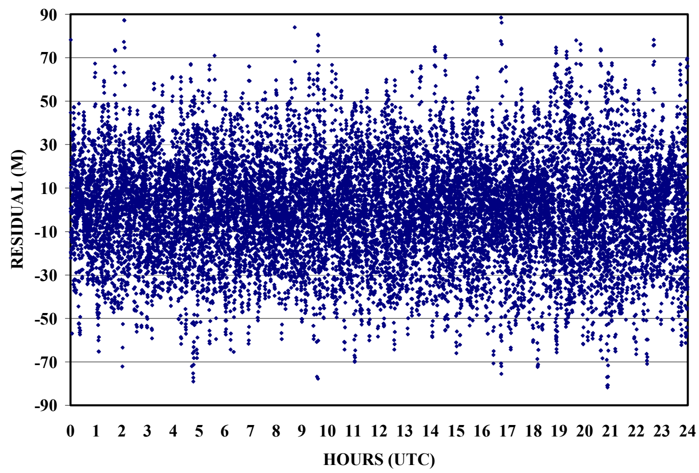

Fig. 3 - Typical behavior of the residuals

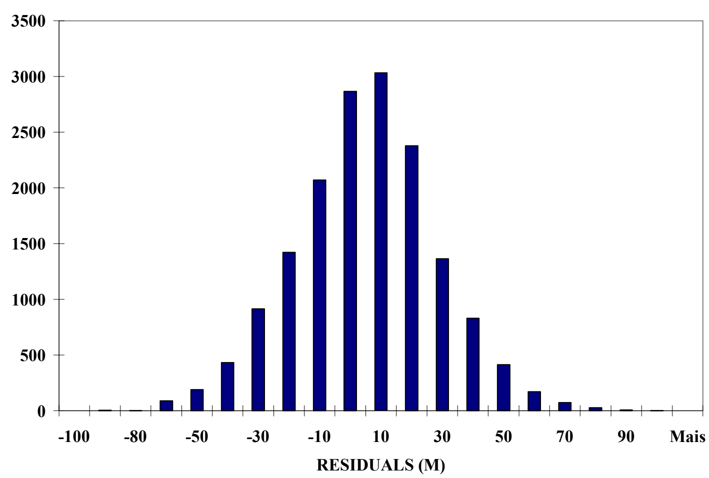

Fig. 4 - Histogram of the residuals

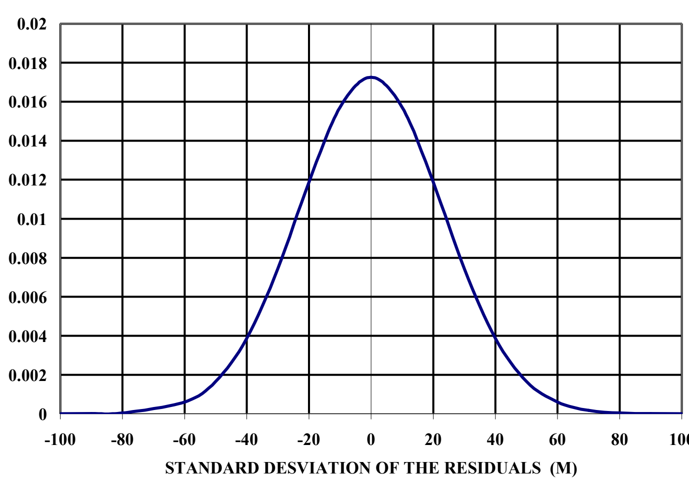

Fig. 5 - Normal distribution of the residuals

TABLE 1 - STATISTICAL ERRORS WITH SA ON OR OFF

DATE MM/DD/YYYY	Δr (m)	Δv (m)	RESIDUALS (m)
11/18/1993	15.5 ± 6,8	0.014 ± 0.006	0.027 ± 13.2
11/19/1993	17.4 ± 6.7	0.016 ± 0.006	-0.13 ± 13.4
11/20/1993	17.6 ± 8.4	0.017 ± 0.007	-0.16 ± 22.6
01/03/1994	16.5 ± 8.5	0.015 ± 0.008	0.004 ± 22.1
01/04/1994	19.5 ± 9.6	0.018 ± 0.009	-0.16 ± 22.8
01/05/1994	19.6 ± 7.8	0.018 ± 0.008	0.04 ± 22.9
01/21/1994	19.0 ± 7.7	0.018 ± 0.008	-0.05 ± 23.9
01/22/1994	16.5 ± 8.6	0.015 ± 0.008	-0.007 ± 23.3